



Research Journal of Pharmaceutical, Biological and Chemical Sciences

Synthesis and Characterization of Sol-Gel Dip Coated Pure and Mn-Doped ZnO Thin Films.

Jonnala Rakesh Reddy, Kovalakannan Sivalingam, Ganesh Kumar Mani, Prabakaran Shankar
and John Bosco Balaguru Rayappan*

Centre for Nanotechnology & Advanced Biomaterials (CeNTAB) and School of Electrical & Electronics Engineering (SEEE) SASTRA University, Thanjavur 613 401, Tamil Nadu, India.

ABSTRACT

Undoped and Mn-doped nanostructured ZnO thin films were deposited on glass substrates using sol-gel dip coating technique and subsequently annealed at 723 K for 3 h. The structural, morphological, optical and electrical properties were investigated. X-ray diffraction patterns confirmed the polycrystalline nature with hexagonal wurtzite structure of ZnO thin films. The crystallite size was found to be decreased with Mn-doping. Scanning electron micrographs showed a closely packed spherically shaped grains distributed uniformly over the film surface. The optical transmittance, band gap and electrical conductivity of the ZnO thin film were decreased with Mn-doping.

Keywords: Sol-gel; ZnO; Thin film; Doping;

**Corresponding author*

INTRODUCTION

Since 1962, metal oxide semiconductor thin films have been on the major focus of the scientists and technologists because of their efficient optical and electrical properties[1]. Among many metal oxide materials, zinc oxide (ZnO) has been dominating during this decade owing to its n-type conductivity with large exciton binding energy of 60 meV and direct energy band gap of 3.36 eV at room temperature[2]. In addition, ZnO is chemically and mechanically stable, abundant in nature, nontoxic, tunable band gap and piezoelectric behaviour. These properties are highly favourable for many applications like short-wavelength light emitting devices, solar cells, field emission devices, chemical and biological sensors, UV lasers, UV detectors, spintronics, etc.

The field of nanoscience and technology has given new dimension in all the sense to this oxide material, which has resulted not only in the number of research articles published per annum but also its presence in the industries and day-to-day life. Further, the phenomena of doping has added crown to ZnO through which one can fine-tune its transport properties by tailoring its band gap. Though there are many attempts have been made to investigate the role of dopants in ZnO, the mechanisms to fine-tune the transport properties of ZnO by doping is still a major concern for scientists and engineers. Among several dopants (Mg, F, B, Cu, Ga, Ni, Co, Cr)[3–6] reported so far, doping manganese (Mn) in ZnO has many unique features since the ionic radii of Mn^{+2} (66 pm) is slightly higher than Zn^{+2} (60 pm). Additionally, introduction of Mn-dopant led to consequential change in size, shape and the band gap of ZnO thin film in-turn led to significant change in the transport properties of ZnO thin film. Caglar *et al.*[7] studied the influence of Mn doping on the inherent properties of sol-gel prepared ZnO thin film and observed a decrease in transmittance and the band gap of ZnO film with Mn-dopants. Sivalingam *et al.* [8] prepared the Mn-doped ZnO thin films using spray pyrolysis technique and observed a change in morphology, decrease in the band gap with increase in Mn-dopant concentration. Nirmala *et al.* [9] observed a decrease in the crystalline quality and band gap of the Mn-doped ZnO films prepared by sol-gel method. Wang *et al.* [10] observed an increase in resistance and the band gap for the sol-gel prepared and post annealed Mn-doped ZnO film. Again, Senthilkumar *et al.* [11] prepared Mn-doped ZnO thin films by sol-gel process and observed the decrease in grain size and band gap. Fukumara *et al.*[12] used the pulse laser deposition method and reported a maximum substitution level of Mn-dopant in ZnO, which was as high as 35% and by maintaining the wurtzite structure of ZnO thin film.

Undoped and Mn-doped ZnO thin films were prepared by various deposition techniques like spray pyrolysis[8], molecular beam epitaxy[13], RF sputtering[14], chemical vapour deposition[15], thermal evaporation[16], sol-gel technique[17], pulsed laser deposition[18], etc. Among them, sol-gel dip coating is unique in-terms of its cost effectiveness and the ability to control the structural and morphological features of the thin films[19]. Hence in the present work, the undoped and Mn-doped ZnO thin films were prepared using sol-gel dip coating technique and their structural, morphological, optical and electrical properties were investigated.

MATERIALS AND METHODS

Thin film deposition

ZnO thin films were deposited on glass substrates using sol-gel dip coating (HOLMARC, HO-TH-02, India) system. Zinc acetate dihydrate ($\text{Zn}(\text{CH}_3\text{COO})_2 \cdot 2\text{H}_2\text{O}$, Sigma Aldrich, 99% purity, USA) and manganese (II) acetate tetrahydrate ($\text{Mn}(\text{CH}_3\text{COO})_2 \cdot 4\text{H}_2\text{O}$, Merck, 99% purity, USA) salts were used to prepare undoped and Mn-doped ZnO thin films. Glass substrates (Blue star, Mumbai) were cleaned ultrasonically (Supersonics, Mumbai) for 15 min using deionized water (Millipore, USA) and acetone and dried for 1 h in the hot air oven. 0.1 M of zinc acetate and 0.002 M of manganese acetate were dissolved in 50 ml of ethanol and stirred ceaselessly for 20 min. Then, 1 ml of monoethanol ammine (MEA) was added and stirred continuously for 15 min. Glass substrates were dipped into the solution with dipping speed of $9000 \mu\text{m}/\text{sec}$ and withdrawal speed of $1000 \mu\text{m}/\text{sec}$ with 1 min duration as dipping time. After each coating, the samples were dried at 78°C for 1 min. Finally, the samples were annealed at 723 K for 3 hours. Fig. 1 shows the optimized parameters used for the preparation of undoped and Mn-doped ZnO thin films.

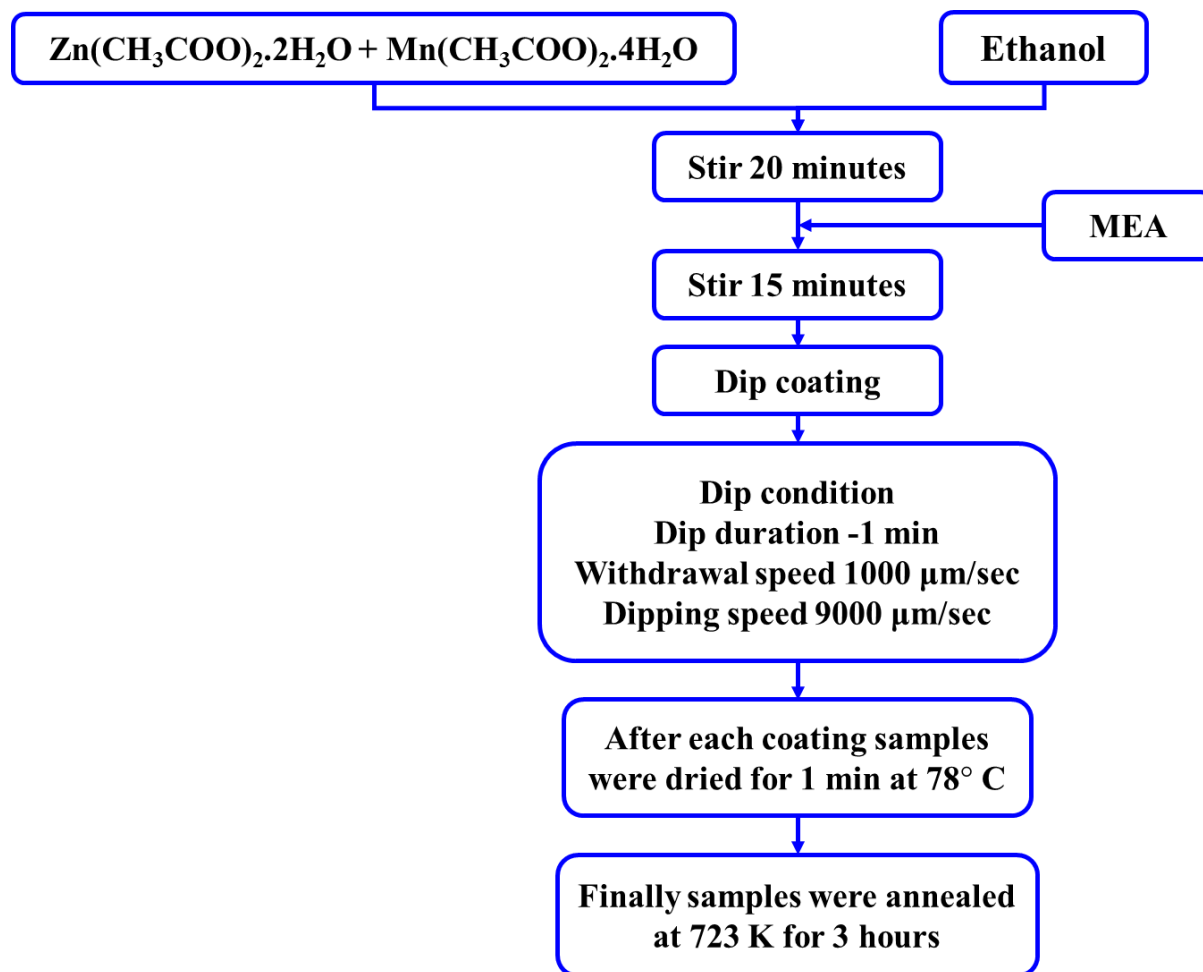


Figure 1: Optimized parameters used for the preparation of undoped and Mn-doped ZnO thin films.

Characterization techniques

Structural characteristics of the ZnO thin films were investigated using X-ray Diffractometer (X'PERT PANalytical, Netherlands) with Cu K α source ($\lambda=1.5408 \text{ \AA}$) in the 2θ range of 10 to 80°. Surface morphologies of the films were studied using Field Emission Scanning Electron Microscope (FE-SEM) (JSM-6701F, JEOL, Japan). Optical properties were observed using UV-Vis spectrophotometer (Perkin Elmer, Lambda 25, USA) in the wavelength range of 350 - 800 nm. Electrical studies were carried out employing a high resistance electrometer (Keithley 6517A, USA).

RESULTS AND DISCUSSION

Structural studies

X-ray diffraction patterns (Fig. 2) of the undoped and Mn-doped ZnO thin films confirmed the polycrystalline nature with hexagonal wurtzite crystal structure. The peaks corresponding to (100), (002), (101) and (110) planes were observed, which are in good agreement with the JCPDS card (no. 36-1451). The absence of secondary peaks corresponding to manganese oxide confirmed the non-influence of Mn-dopants in the hexagonal wurtzite structure of ZnO film. Decrease in peak intensity was observed when Mn was doped in ZnO [20]. A slight decrease in lattice parameters and intensity of Mn-doped ZnO film compared to undoped ZnO might be due to the higher ionic radius of Mn⁺² (66 pm) compared to Zn⁺² (60 pm) [21]. The average crystallite size of the undoped and Mn-doped annealed ZnO thin films was calculated using Debye Scherrer formula given (Eq. 1.)

$$D = \frac{0.9\lambda}{\beta \cos\theta} \quad (1)$$

where ' λ ' is the wavelength of the X-ray used (1.5406 Å for Cu K α), ' θ ' is the Bragg's angle and ' β ' is the full width at half maximum. Crystallite size was found to be decreased for Mn-doped ZnO film (Table 1). Strain was found to be increased in the Mn-doped ZnO film, which was calculated using the formula given in Eq. 2.

$$\varepsilon = \frac{\beta}{4 \tan\theta} \quad (2)$$

where, ' ε ' is the strain, ' β ' is the full width at half maximum and ' θ ' is the Bragg's angle. The dislocation density was increased in the Mn-doped ZnO lattice. Where the dislocation density (δ) gives the information about crystal structure. The dislocation density is the length of dislocation lines per unit volume of the crystal, which is given in Eq. 3.

$$\delta = \frac{1}{D^2} \quad (3)$$

where 'D' is the crystallite size of thin film. The obtained dislocation density values for undoped and Mn-doped ZnO films are given in Table 1. Specific surface area of the undoped and Mn-doped ZnO films was calculated using the equation (Eq. 4) given below:

$$A = \frac{6}{D \times \rho} \quad (4)$$

where, 'A' is the specific surface area, 'D' is the estimated crystallite size and 'ρ' is the density of ZnO (5.606 g m⁻³). The estimated parameters from XRD data are given in Table 1. Increase in surface area might be due the prevention of crystal growth by dopant ions and inhibit between grains during heat treatment [22,23].

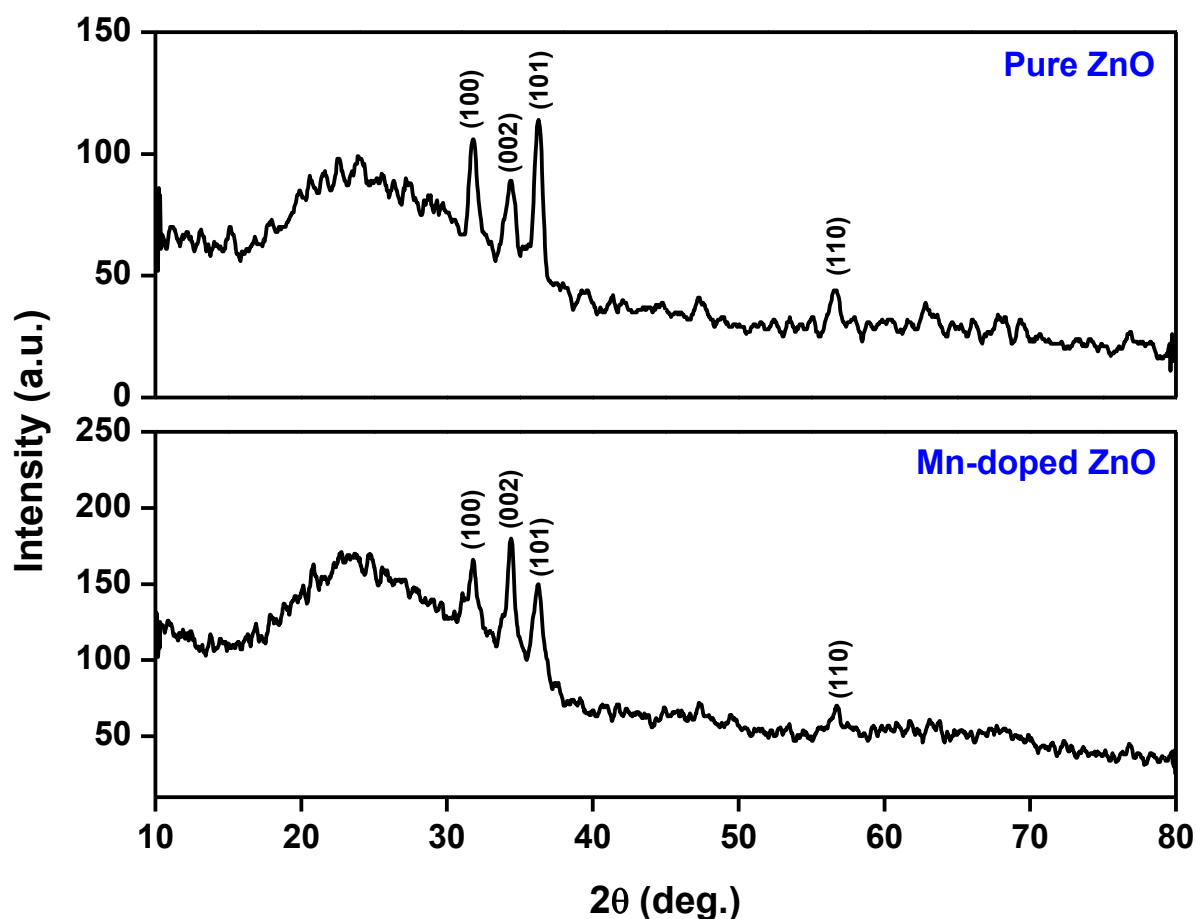


Figure 2: X-ray diffraction patterns of the undoped and Mn-doped ZnO thin films.

Morphological studies

Scanning electron micrographs (Fig. 3 (a) & (b)) of the undoped and Mn-doped ZnO thin films showed a uniformly distributed spherical shaped tightly packed grains distributed over the film surface without any voids and cracks. Decrease in grain size of the ZnO film was observed with Mn-doping. This might be due to the creation of zinc interstitials during the growth of ZnO

grains. By doping Mn in ZnO, the diffusivity of Zn might have decreased, which resulted in the suppressed grain growth of the Mn-doped ZnO film compared to that of undoped film[24].

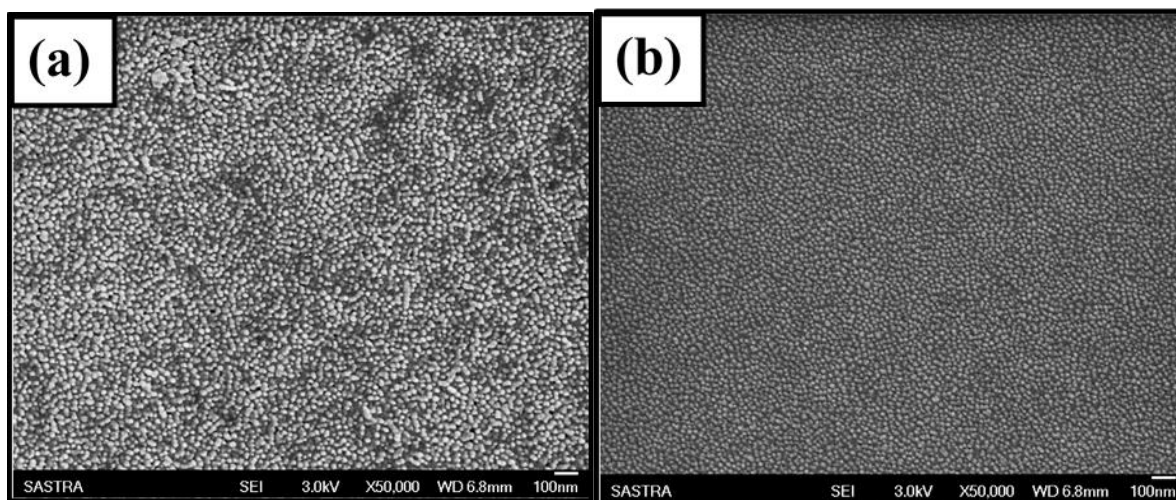


Figure 3: Scanning electron micrographs of the a) undoped and b) Mn-doped ZnO thin films.

Optical properties

The optical transmittance (Fig. 4(a)) and absorbance (Fig. 4(b)) spectra showed the decrease in transmittance of the Mn-doped ZnO film, which may be due to the formation of new energy states by Mn substituents and these new defect states might have absorbed the additional photon energy[25]. Kim *et al.* reported that the increase in absorption was due to the absorption of higher-energy photons and subsequent energy exchange interactions between the electrons of the host and dopant atoms [26]. Fig. 4(c) shows the graph plotted between $h\nu$ and $(\alpha h\nu)^2$. Band gap of the undoped and Mn-doped ZnO films were calculated using the absorbance spectra and Tauc's equation (Eq. 5.),

$$\alpha h\nu = A(h\nu - E_g)^n \quad (5)$$

where ' α ' is the absorption coefficient, ' $h\nu$ ' is the photon energy, E_g is the optical band gap energy and ' A ' is the constant, where $n = 1/2$ for allowed transitions, $n = 2$ for allowed indirect transitions, $n = 3/2$ for forbidden direct transitions and $n = 3$ for forbidden indirect transitions. Decrease in band gap of Mn-doped ZnO film (2.9 eV) was observed compared to that of undoped ZnO film (3.05 eV). This might be due to the exchange interactions between the *sp*-orbital electrons of host and dopant atoms and the same was reported as an effect second-order perturbation and low dimensionality of the materials[27,28].

Electrical studies

The electrical resistance of the undoped and Mn-doped ZnO films were measured using the high resistance electrometer (Keithley 6517A, USA). The resistance of the

ZnO film was found to be increased with Mn doping from $7.2 \times 10^{10} \Omega$ to $3.16 \times 10^{11} \Omega$. The increase in resistance of the ZnO film with Mn doping might be due to the decrease in crystallite size. Decrease in crystallite led to the enrichment of number of grain boundaries and hence grain boundary scattering[29]. Moreover, Plugaru *et al.* reported that the increase in electrical resistance of the Mn-doped ZnO film due to the suppression of intrinsic impurities in the host ZnO film by Mn dopants[30].

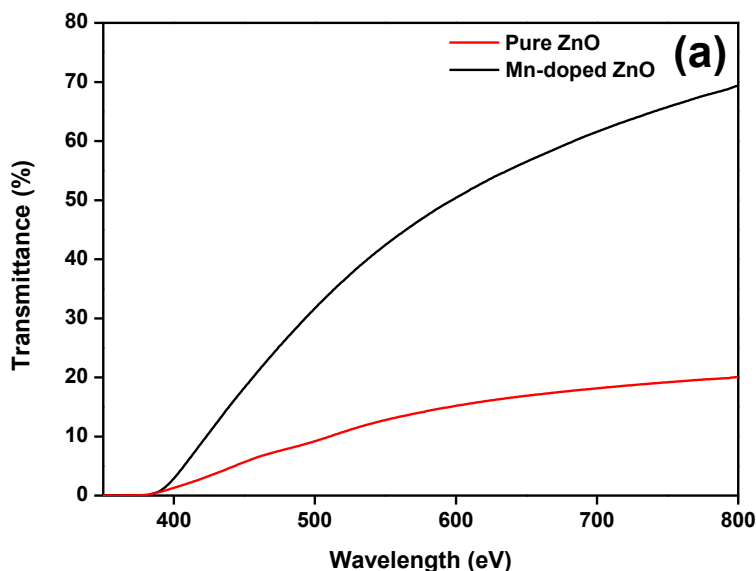


Figure 4(a): Optical transmittance spectra of the undoped and Mn-doped ZnO thin film.

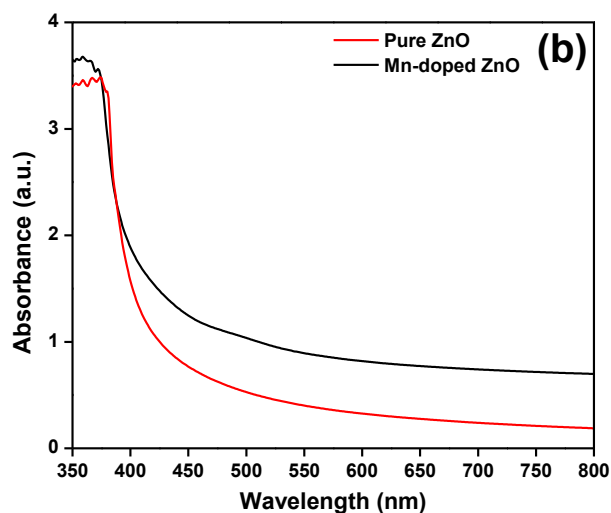


Figure 4(b): Optical absorbance spectra of the undoped and Mn-doped ZnO thin film.

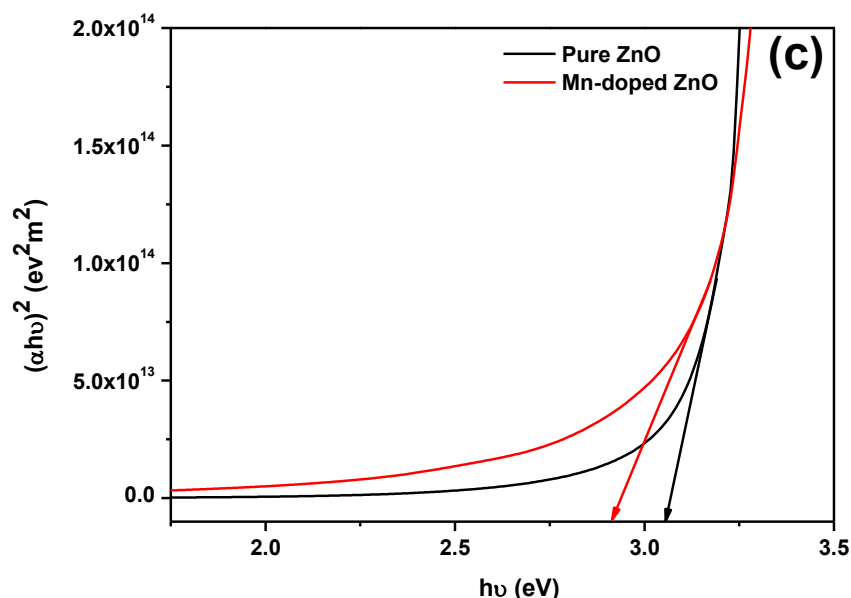


Figure 4(c): Graph plotted between $h\nu$ and $(\alpha h\nu)^2$ for the undoped and Mn-doped ZnO thin films.

Sample	Crystal Plane	Crystallite Size (nm)	d-spacing (Å)	Strain	Dislocation Density $\times 10^{15}$ (Line ² /m ²)	Specific Surface Area m ² /kg
Pure ZnO	100	22.14	2.81	0.0016	2.03	4.83
	002	24.32	2.60	0.0014	1.68	4.39
	101	22.41	2.47	0.0016	1.99	4.77
Mn-doped ZnO	100	17.54	2.80	0.0020	3.24	6.10
	002	14.71	2.60	0.0024	4.61	7.27
	101	14.79	2.46	0.0024	4.56	7.23

Table 1: Estimated structural parameters.

CONCLUSION

The influence of Mn doping on the structural, morphological, optical and electrical properties of ZnO thin films were studied. X-ray diffraction patterns revealed the doping of Mn into ZnO lattice without altering the hexagonal wurtzite crystal structure of ZnO. Crystallite size of the ZnO film was found to be decreased with Mn-doping. Scanning electron micrographs showed a closely packed spherically shaped grains distributed all over the film surface. Optical studies showed the decrease in transmittance of the ZnO film with Mn doping. Band gap of the ZnO film was decreased with Mn doping due to *sp-d* exchange interactions. Electrical studies revealed that Mn-doping increased the resistance of the ZnO thin film.

ACKNOWLEDGEMENTS

The authors wish to express their sincere thanks to the Department of science & Technology, New Delhi, India for their financial support (ID: INT/SWD/VINN/P-04/2011 and SR/FST/ETI-284/2011(C)). They also wish to acknowledge SASTRA University, Thanjavur for extending infrastructure support to carry out this work.

REFERENCES

- [1] JLG Fierro. Metal Oxides: Chemistry & Applications. Taylor & Francis, 2005, pp. 1-5.
- [2] K Vijayalakshmi, K Karthick. J Mater Sci Mater Electron 2013; 24: 2067–2071.
- [3] H Benzarouk, A Drici, M Mekhnache, A Amara, M Guerioune, JC Bernède, H. Bendjffal. Superlattices Microstruct 2012; 52: 594–604.
- [4] CY Tsay, WC Lee. Curr Appl Phys 2013; 13: 60–65.
- [5] M Babikier, D Wang, J Wang, Q Li, J Sun, Y Yan, Q Yu, S Jiao. Nanoscale Res Lett 2014; 9: 199.
- [6] M. Ebrahimizadeh Abrishami, A Kompany, SM Hosseini, N Ghajari Bardar. J Sol-Gel Sci Technol 2012; 62: 153–159.
- [7] Y. Caglar, S. Ilican, M. Caglar, F. Yakuphanoglu. J. Sol-Gel Sci. Technol. 2009; 53: 372–377.
- [8] D. Sivalingam, J. B. Gopalakrishnan, J. B. B. Rayappan. Sensors Actuators B Chem. 2012; 166: 624–631.
- [9] M Nirmala, A Anukaliani. Photonics Lett Pol 2010; 2: 189–191.
- [10] J Wang, W Chen, M Wang. J Alloys Compd 2008; 449: 44–47.
- [11] S Senthilkumar, K Rajendran, S Banerjee, TK Chini, V Sengodan. Mater Sci Semicond Proc 2008; 11: 6–12.
- [12] T Fukumura, Z Jin, M Kawasaki, T Shono, T Hasegawa, S Koshihara, H Koinuma. Appl Phys Lett 2001; 78: 958.
- [13] M Ebrahimizadeh Abrishami, A Kompany, SM Hosseini, N Ghajari Bardar. J Appl Phys 2012; 112: 5.
- [14] M Ebrahimizadeh Abrishami, A Kompany, SM Hosseini, N Ghajari Bardar. Mater Lett 2008; 62: 3379–3381.
- [15] JJ Liu, MH Yu, W. Zhou. Appl Phys Lett 2005; 87: 172505.
- [16] Lian Feng, Zheng Kai Hong, Liu Zheng, Liu Ji, Hu Li Jun, Wang DongWei, Chen Chun Ying, Sun. Chinese Phys B 2010; 19: 172505.
- [17] K Omri, J El Ghoul, OM Lemine, M Bououdina, B Zhang, L El Mir. Superlattices Microstruct 2013; 60: 139–147.
- [18] Q Li, Y Wang, J Liu, W Kong, B Ye. Appl Surf Sci 2014; 289: 42–46.
- [19] CJ Brinker, GW Scherer. Sol-gel Science: The Physics and Chemistry of Sol-gel Processing. Academic Press, 1990, pp. 908.
- [20] AG Ali, FB Dejene, HC Swart. Cent Eur J Phys 2011; 10: 478–484.
- [21] J Elanchezhian, KP Bhuvana, N Gopalakrishnan, T Balasubramanian. Mater Lett 2008; 62: 3379–3381.
- [22] V Bhavanasi, CB Singh, DDatta, V Singh, K Shahi, S Kumar. Opt Mater 2013; 35: 1352–1359.



- [23] W Lojkowski, et al. J Nanoparticle Res 2008; 11: 1991–2002.
- [24] T Tsuzuki, Z Smith, A Parker, R He, X Wang. J Aust Ceram Soc 2009; 45: 58–62.
- [25] R Karmakar, SK Neogi, A Banerjee, S Bandyopadhyay. Appl Surf Sci 2012; 263: 671–677.
- [26] VR Shinde, TP Gujar, CD Lokhande, RS Mane, S-H. Han. Mater Chem Phys 2006; 96: 326–330.
- [27] KJ Kim, YR Park. Appl Phys Lett 2002; 81: 1420.
- [28] RB Bylsma, WM Becker, J Kossut, U Debska, D Yoder-Short. Phys Rev B 1986; 33: 8207–8215.
- [29] P Singh, A Kaushal, D Kaur. J Alloys Compd 2009; 471: 11–15.